CHALMERS

Self-assembly of class II hydrophobins on highly polar surfaces

Master of Science Thesis in the Master Degree Programme Biotechnology

MATHIAS S. GRUNÉR

Department of Chemical and Biological Engineering

Division of Life Sciences

CHALMERS UNIVERSITY OF TECHNOLOGY

Gothenburg, Sweden, 2011

Self-assembly of class II hydrophobins on highly polar surfaces

MATHIAS S. GRUNÉR, 2011

Work perfomed at:
VTT Technical Research Centre of Finland,
Nanobiomaterials,
Espoo, Finland

Performed as part of:
Master Degree Programme Biotechnology
Department of Biotechnology
Chalmers University of Technology
SE-412 96 Gothenburg
Sweden
Telephone + 46 (0)31-7721000

Supervisor:
Professor Markus B. Linder
Nanobiomaterials,
VTT Technical Research Centre of Finland

Examiner:
Professor Christer Larsson
Department of Chemical and Biological Engineering
Division of Life Sciences
Chalmers University of Technology

Self-assembly of class II hydrophobins on highly polar surfaces

MATHIAS S. GRUNÉR, 2011

Department of Chemical and Biological Engineering

Chalmers University of Technology

Abstract

Hydrophobins, adhesive proteins produced by filamentous fungi, have been described as the most surface active proteins known and show extraordinary properties regarding formation of surfaces. Hydrophobins have roles in the growth and development of the fungi including function in adhesion to surfaces, reducing surface tension for aerial growth and spore hydrophobicity and to aid spreading of aerial spores. Observations of filamentous fungi show that the structures formed by their mycelia can be very hydrophobic. Furthermore, airborne spores (conidia) covered with a surface layer of hydrophobin has been shown to mask the recognition of the conidia by the human immune system and hence prevents immune response. The knowledge of how hydrophobins aid in producing these fascinating properties is far from complete. This study aims to explain this by examining the abilities of the class II hydrophobins HFBI, HFBII and HFBIII to bind to submerged polar surfaces making them more hydrophobic, replicating the role hydrophobins have when forming hydrophobic surface coatings by self assembly on fungal spores and mycelia of filamentous fungi. It is shown here that binding onto submerged polar surfaces occurs by self assembly under specific conditions and that the binding can result in a significant increase in water contact angle of the surface, hence making it more hydrophobic.

Keywords: Hydrophobins, class II, self-assembly, water contact angle, QCM-D, hydrophobicity, RESI

Abbreviations:

HEX: 1-Hexanethiol

TMA: Trimethylamine thiol

PEI: Polyethyleneimine

MUA: 11-Mercaptoundecanoic acid

SAM: Self Assembled Monolayer

QCM-D: Quartz Crystal Microbalance with Dissipation

RESI: Resonance Enhanced Surface Impedance

WCA: Water Contact Angle

Table of Contents

1 Introduction

Hydrophobins, adhesive proteins produced by filamentous fungi, have been described as the most surface active proteins known[1] and show extraordinary properties regarding forming membranes at interfaces. Hydrophobins have roles in the growth and development of the fungi including function in adhesion to surfaces, reducing surface tension for aerial growth and spore hydrophobicity and to aid spreading of aerial spores.[2] Hydrophobins are amphiphilic molecules that assemble into membranes at different interfaces through self-assembly. Observations of filamentous fungi show that the structures formed by their mycelia can be very hydrophobic (Figure 1). Furthermore, airborne spores (conidia) covered with a surface layer of hydrophobin has been shown to mask the recognition of the conidia by the human immune system and hence prevents immune response[3]. The knowledge of how hydrophobins aid in producing these fascinating properties is far from complete. This study aims improve our understanding on this by examining the abilities of the hydrophobins HFBI, HFBII and HFBIII to bind to submerged polar surfaces making them more hydrophobic, replicating the role hydrophobins have when forming hydrophobic surface coatings by self assembly on fungal spores and mycelia of filamentous fungi. This is examined mainly by Quartz Crystal Microbalance with Dissipation (QCM-D) as well as Water Contact Angle (WCA) measurements.

Hydrophobins are divided into two classes, class I and class II, based on the occurrence of hydrophilic and hydrophobic amino acid residues in the protein sequence[4]. The hydrophobins used here belong to class II and have essential roles in the growth and development of the fungus *Trichoderma reesei*, including function in cell wall and spore hydrophobicity[2,5] Previously, studies of hydrophobin membranes at the air-water interface and on hydrophobic surfaces have been carried out [6-11], but there is no published work on how hydrophobins can bind to a polar surface making it more hydrophobic. It is shown here that binding onto submerged polar surfaces occurs by self assembly under specific conditions and that the binding can result in a significant increase in water contact angle of the surface, hence making it more hydrophobic. In these cases, charged residues opposite of the hydrophobic patch of the amphiphilic proteins are thought to interact with the solid polar surface in such a way as the hydrophobic patch is turned outwards against the solution resulting in a hydrophobic surface coating. The results found here are also

important in an commercial point of view, since in biotechnological industry, hydrophobins are today facing a large interest for industrial applications[12] and are mentioned as having possible uses in e.g. drug delivery, biomedical implants, cell- and protein immobilizing, foam stability and development, surface modifications, and biosensing.[13] A large number of patent applications have been filed concerning hydrophobins and several industry leading companies are taking interest and performing research on the use and function of these proteins. Recently a growing interest has been shown in general on hydrophilic to hydrophobic surface transformations. [9,13,14]

This thesis presents the subject described above starting with a thorough introductory chapter. Firstly, the theory behind hydrophobicity is presented including the presence of hydrophobic phenomena in nature and theory of protein-surface interactions. This is followed by a comprehensive description of hydrophobins; their biological function, structure, properties, applications and previous research in the ability of the proteins to alter surface hydrophobicity.

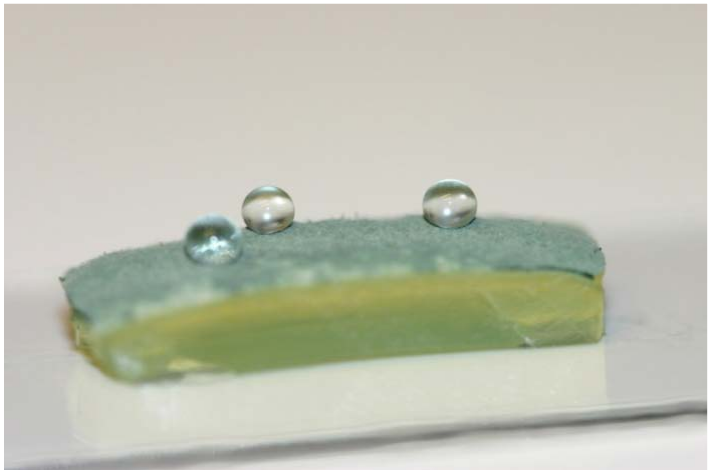

Figure 1 The surface of a mycelial mat of *T. reesei* growing on agar is highly hydrophobic as shown by water contact angles of about 140°

1.2 Hydrophobicity

1.2.1 Theory of hydrophobicity

1.2.1.1 Wetting and WCA

The behavior of liquids on solid substrates can be described by wetting.[15] Different liquids deposited on the same surface can behave very differently and e.g. aqueous droplets deposited on different substrates can show remarkable difference in behavior. The wetting behavior can be described by the water contact angle, WCA. The water contact angle is easily measured and is a very useful indicator of the wetting, or hydrophobic/hydrophilic properties of a material.[15,16] The angle a liquid makes with a solid is defined as the static contact angle, θ_0. Roughly speaking, a wetted solid is referred to as hydrophilic and a nonwetted solid is called hydrophobic. Surfaces with contact angles lower than 10° are referred to as superhydrophilic and surfaces higher than 150 are referred to as superhydrophobic. [15-17] The WCA is a method of presenting the energy of a surface and is also affected by the cleanness or roughness of the surface. [15,16]

When depositing droplets on surfaces three different wetting cases can be distinguished, nonwetting, partial wetting and complete wetting[15]. Nonwetting behavior can be seen when attempting to form a layer of mercury on a glass surface. When this is tried, the mercury immediately forms a droplet where the contact with the glass is minimized to a spherical cap with a contact angle larger than 90°. On the same glass surface it is however easily possible to make a covering oil layer by spreading an oil droplet completely on the glass. In this case, the contact angle decreases to zero within time and the wetting is described as complete wetting. Partial wetting can be seen on a glass surface when e.g. a droplet of water is deposited. In this case the contact angle varies between zero and 90° and thus, a water droplet on glass behave in a manner that is intermediate between water and oil. However, when depositing a water droplet on Teflon, it will be unable to form a complete layer, similar to the way mercury behaves on glass. This is an example of how wetting and nonwetting is a property of the liquid-solid pair and not singly the liquid. A non wetting liquid forming a sessile drop on the surface of a solid forms a three phase line, TPS, at which all three phases , solid, liquid and vapor are in contact. The static contact angle θ_0 can be expressed by the Young equation, , where

is the surface-drop interfacial tension, is the surface-vapor interfacial tension and the drop- vapor interfacial tension.[18] (Figure 2)

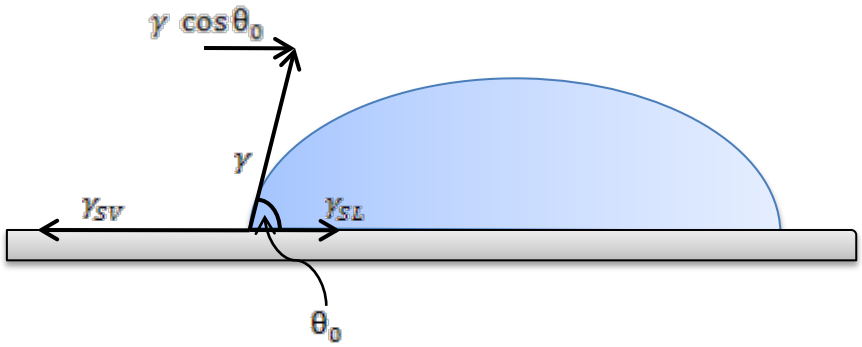

Figure 2 Two-dimensional representation of a drop on a surface describing interfacial tensions as described by the Young equation. Represents the surface-drop interfacial tension, is the surface-vapor interfacial tension and the drop- vapor interfacial tension.

1.2.1.2 Hydrophobic effect

The Hydrophobic effect of a surface can be described regarding the arrangement of water molecules around the surface.[19] Water molecules can adopt orientations around a small hydrophobic particle that allows them to go around the molecule and structure via hydrogen bonding. In this case, each water molecule can participate in four hydrogen bonds with other water molecules when covering the small molecule, which is the same amount of hydrogen bonds they have in solution. A larger surface made of the same particles is however not allowing water molecules to adopt around due to the size of the surface. The water molecules are unable to maintain a complete hydrogen bonding network with the surrounding liquid. As a result of this sacrifice of hydrogen bonds, water molecules tends to move away from this surface, which now can be described as hydrophobic. [19] The formation of a hydrophobic surface via self assembly of hydrophobins in solution can be described via this effect.

1.2.1.3 Hysteresis

In many surfaces the real WCA is hysteric, that is it renders different values of WCA whether the liquid drop is increasing or decreasing on the surface, and the three phase line is moved. [18,20] In some cases, the angles can vary as much as 60°. This phenomenon is the contact angle hysteresis. Hysteresis can arise from molecular interactions between the liquid and solid or from surface anomalies, such as roughness or heterogeneities of the surface[20]. A low hysteresis can be

seen on a surface where a water droplet rolls of a surface with a small change in advancing and receding WCA. A higher hysteresis value is found for a more sticky and uneven surface where the drop does not roll of easily with the liquid of choice. The hysteric CA is normally used regarding superhydrophobic surfaces as a complementary description.

1.2.1.4 Heterogeneous and homogenous wetting

Regarding wetting and roughness of the surface, one of the most central questions is if the liquid fills up the roughness grooves of the solid. The wetting is called heterogeneous if air is trapped in these grooves underneath the liquid drop, and homogeneous of that is not the case. These two types of wetting regimes have been subjects of vast studying and was established by Wenzel, for the homogenous wetting ("Wenzel drop") and by Cassie and Baxter ("Cassie drop") for the heterogeneous wetting regime. [21]Both of these models explain how a drop with a high WCA can be formed to render surfaces with high hydrophobicity as described in the next chapter.

1.2.2 Hydrophobicity in nature

In nature, hydrophobic surfaces can be found in e.g. plants, insects and animals.[17,22] In the 1990s, the research of natural hydrophobicity started focusing on superhydrophobic surfaces, including water repellant leaves from e.g. *Nelumbo nucifera* (Lotus) showing high water contact angels above 140.°[17,22,23] The surface of leafs with superhydrophobic properties have a micro scale roughness as a result of papillose epidermal cells forming microasperties or papillae. These papillae are themselves displaying a roughness in the nanoscale. Asperties formed by three dimensional epicutular hydrophobic long chain hydrocarbons, wax crystals, creating a superhydrophobic entity. On Lotus leaves these wax crystals exist as tubules, and on other leaves they can form e.g. platelets. The superhydrophobic properties of these leaves is created as air bubbles fill the "valleys" of the structure and water droplets sit on the peaks of the nanostructure. The static contact angle of a water droplet on a lotus leaf can reach angles over 160° and hysteresis of only 3°. [17,22]The high WCA in combination with a low hysteresis, where the drop rolls of the surface of the leaf, has the result that the water droplet removes any contaminant particle of the surface of the drop, a so called self-cleaning.

Gao *et al.*[24] examined the hydrophobicity of the legs of the water strider (*Gerris remigis*) which is able to run on water. The authors found that a leg of the water strider generates contact angels of 167.6 ± 4.4° and that a special hierarchical structure of the legs is responsible for the

hydrophobicity. On the legs, a large number of tiny hairs, microsetae, with fine nanogrooves are situated. The setae are needle shaped, with diameters from 3 μm to a few hundred nm, about 50 μm in length and arranged at an inclined angle of 20°. Air is trapped in various spaces in the setae and the grooves form a cushion at the leg-water interface in a Cassie type of way preventing the legs from being wetted and generating superhydrophobicity. The total supporting force of a leg is about 15 times the body weight of the insect. [24]

Yang *et al.*[25] showed that the antifogging properties of mosquito eyes is a result of the superhydrophobic surface structure of the eye. The authors found hundreds of hexagonally close packed hemispheres at the microscale called ammatida which function as individual sensory units and have a diameter of about 26 mm. At the nanoscale, each ammatida is covered with nanonipples with an average diameter of 101 nm that arrange in a hexagonal non close packed array. This hierarchical structure results in the superhydrophobicity of the eye.

1.3 Protein - surface interactions

Interactions between proteins and surfaces is an important factor in many natural processes. In biological environment, the surface of a material is coated within seconds by proteins which in turn modulates cell attachment, spreading and migration[26]. Following this, protein adsorption to surfaces has an important role in e.g. regenerative medicine, tissue engineering and drug delivery systems.[26] The protein adsorption on surfaces can be controlled by external factors, mainly temperature, ionic strength and buffer composition.[26] Protein adsorption to a surface can be described by the Gibbs free energy equation. For adsorption to occur and the surface-protein-solution system to reach the minimum equilibrium potential the Gibbs free energy should decrease; . The major driving force of protein adsorption is a gain in entropy caused by release of water molecules and salt ions adsorbed on the surface as well as possible structural arrangement inside the protein.[27] Following this, the amount of adsorbed proteins to a surface generally increases at elevated temperatures.[27] The electrostatic state of a protein varies with pH. When the pH and the isoelectric point, pI, are equal the net charge of the protein is zero and the numbers of positive and negative charges of the protein are in balance.[26,27] At pHs below the pI the protein has a net positive charge and above a net negative. At the pI the electrostatic protein-protein repulsions are minimized which can allow higher packing densities

of the protein on the surface.[26] Adsorption rates are however high when the protein and surface have opposite charges. Ionic strength, the concentration of dissolved ions in the solution, is another parameter controlling protein adsorption.[26,28] The higher the ionic strength, the shorter the electrostatic interactions between charged entities are. As a result, at increased ionic strength the adsorption of charged proteins or protein domains to an oppositely charged surface is decreased. If the protein charge and surface charge are repulsive, increased ionic strength is however increasing binding.[28]

When adsorbing to a substrate or surface, size, structural stability and composition can be used to classify the behavior of the proteins.[29] Small and rigid proteins can be seen as hard and have a low tendency to undergo changes in their structure after adsorption which can be the case for intermediate size proteins that are more likely to undergo conformational reorientations after surface adsorption. Hydrophobins are small proteins that are very stable due to their extended network of disulfide bonds that stabilize the structure and essentially form the core of the protein.[30]

Proteins usually exhibit different affinities at different regions of their surfaces depending on the composition of displayed amino acid residues.[26] Commonly, the surface of proteins can be divided into patches with different properties, hydrophobic, hydrophilic or positive or negative charge.[26] A protein will generally expose a possible hydrophobic patch to a hydrophobic surface and its hydrophilic to a hydrophilic one. Proteins adsorbing on positively or negatively charged interfaces normally expose oppositely charged regions to the surface.[26]

1.4 Hydrophobins

Hydrophobins, adhesive proteins produced by filamentous fungi, have been described as the most surface active proteins known[1] and show extraordinary properties regarding formation of surfaces. This group of proteins can be divided into two classes, class I and class II.[4] The classification was made after the discovery o the first genes of hydrophobins which were found when searching for abundantly expressed genes during the development of the fungi *Schizophyllum commune.* [4] In order to evaluate the hydrophilicity and hydrophobicity of the proteins a hydrophaty scale[31] was used and based on the occurrence of hydrophilic and hydrophobic amino acid residues in the protein sequence the classification of the two classes was made. The authors found that the proteins were relatively small, 10 kDa and contained a large

proportion of hydrophobic amino acids. Up to date, class II hydrophobins have only been observed in Ascomycetes while class I hydrophobins are found both in Ascomycetes and Basidomycetes.[30] The sequence of hydrophobins of both classes typically includes eight cystein residues in a specific pattern, where the second and third and sixth and seventh residues always are neighbors in sequence forming a pair[30] . Other amino acid residues in the proteins are otherwise diverse. Due to the strongly similar pattern of the cystein regions it is suggested that all hydrophobins of all classes would share a common disulfide network and as a result, a common fold[30] The authors further suggested that the overall low sequence conservation indicates that the conserved cystein regions are important for structural reasons whereas the other residues can vary and result in specific properties of the different hydrophobins. Fungi normally have genes for several different hydrophobins. Hydrophobins can be found in the cell wall, coating of spores, fruiting bodies as well as in the surrounding medium of the fungi[13,30,32]. Below the biological function, properties, structure and applications of hydrophobins will be presented followed by a thorough description of previous research in the ability of the proteins to alter surface hydrophobicity.

1.4.1 Biological function

1.4.1.1 Spores and hyphea

Mature fungal spores generally have a hydrophobic surface that protects them from wetting or drying and aids their dispersal. By disrupting genes encoding hydrophobins present in the spores, loss of spore hydrophobicity has been shown for both class I[33-35], and class II[36] hydrophobins. HFBI and HFBII have essential roles in the growth and development of the fungus *T. reesei*. HFBI was found to be located in cell walls and HFBII in the spore walls[2,5] By gene disruption, HFBII has been shown to have a role in spore hydrophobicity and to aid spreading of aerial spores[2]. HFBI facilitates aerial growth and has been found in vegetative submerged hyphae of *T. reesei*[37]. The class I hydrophobin Sc3p has been shown to exist in aerial hyphae of *S. commune*[14] making them hydrophobic and ABHI of *Agaricus bisporus* has been found as rodlets on the fruiting bodies of the fungus with hydrophobicity as a result[6]. Aimanianda *et al.*[3] showed that airborn spores (conidia) of *Aspergillus fumigatus* are covered with a surface rodlet layer of the class I hydrophobin RodA and that this layer masks the recognition of the conidia by the human immune system and hence prevents immune response. The hydrophobic effect of these proteins

in their natural role makes them very interesting subject for the hydrophilic-hydrophobic transformations examined in this work. Keyhani *et al.*[38] showed that deletion of the class I hydrophobin genes hyd1 and hyd2 of the entomogenous filamentous fungus, *Beauveria bassiana* generated rodletless or partly covered conidia, respectively, with decreased spore hydrophobicity. The class I hydrophobin SC4 was found to line the gas channels of the fruiting bodies of *S. commune*[10] and to be preventing these channels to be filled with water[39] The class I hydrophobin SC3 have also been shown to affect cell wall composition of hyphae of *S. commune* by influencing the linkage of glucan to chitin[40].

1.4.1.2 Fruiting bodies

The class I hydrophobin ABHI, of *A. bisporus* has been shown to be fruiting body specific. [41] The mRNA of the gene hypA, coding ABHI, was found to accumulate in the pilepeilis (peel) of the mushroom caps where it constitutes more than 60 % of the mRNA population as found by De Groote *et al.* [41]. The ability of ABHI to form hydrophobic surfaces has been shown by Lugones *et al.*[6] and as a results the authors propose that ABHI is the major constituent of the hydrophobic layer surrounding the caps of the fruiting body of *A. bisporus.*

1.4.1.3 Formation of surface membranes

Filamentous fungi form sexual and asexual reproductive structures, such as mushrooms, and thereby grow into the air.[1] In order to do this, they need to cross the barrier of the water surface tension between the moist growing substrate and the air. In order to do this the fungi secretes hydrophobins, as described by Wösten *et al.*[1], who examined the filamentous fungi *S. commune.* The authors described how the fungi reduced water surface tension in order for its hyphae to escape the aqueous phase. The authors measured a large drop in surface tension (72 to 24 mJ m–2) and showed that this drop was caused by self assembly of the secreted hydrophobin SC3. The hydrophobin forms a stable amphiphilic film in the air-water interface and the authors concluded that the hydrophobin first lowers the surface tension of the surrounding water of the hyphae allowing them to emerge from the liquid and as a second step coats the aerial hyphae with a hydrophobic wall enabling the hyphae to grow into the air. These finding also indicated that the proteins are amphiphilic.[30,42] Amphiphilic molecules present distinct hydrophilic and hydrophobic parts which give them special properties including the ability to migrate to hydrophobic- hydrophilic interfaces as well as the ability to encapsulate and dissolve

hydrophobic molecules into aqueous media.[43] Also, amphiphiles can have a major part in self-assembly. Later, values of surface tension of water after addition of hydrophobin ranging from 45 to 27 mNmmNm−1 have been reported.[8,44] The results are depending on the hydrophobin type and concentrations used. Cox *et al.*[45] used the Wilhelmy plate technique and could measure a maximal reduction of surface tension at 25 mN m-1 by using the class II hydrophobins HFBI and HFBII. The authors further showed that there was a clear break in the curve of protein concentration versus surface tension at a protein concentration of 0.38 μM which was described as the surface saturation constant.

1.4.2 Properties

1.4.2.1 Rodlets

Rodlet formation was discovered early on in the research of class I hydrophobins. These formations are so far only observed in vitro and are typically seen when a drop of dilute hydrophobin is allowed to dry down on a solid support.[6,46] Characteristic rodlets in electron microscopy and atomic force microscopy has been found when allowing a solution of hydrophobin to dry down on a solid surface.[4,14] Wösten *et al.*[14] allowed the class I hydrophobin Sc3p to dry down on a hydrophilic surface and found that the protein spontaneously assembled into an SDS-insoluble protein membrane on the surface. This effect was also seen on the surface of gas bubbles. Electron microscopy showed rodlets spaced 10 nm apart which were similar to rodlets formed on aerial hyphae and was described as hydrophobic.

1.4.2.2 Foaming

Sarlin *et al.*[47], decribes the effect of beer gushing, where beer gushes out of a bottle after opening even without shaking the bottle before opening. Hydrophobins from *Fusarium, Nigrospora* and *Trichoderma* have been proven as gushing factors in beer by the authors. Hydrophobin in concentrations as low as 0.003 ppm was shown to be sufficient to induce gushing of beer in a 33 cl bottle.

1.4.2.3 Behavior in solution

Aggregates of Class I hydrophobins only dissolve in strong acids such as TFA, whereas aggregates of class II hydrophobins can be dissolved much more easily in aqueous dilutions of organic solvents.[30] Hydrophobins have been shown to form different dimers and oligomers in

solution. The formation of multimers is explained by the amhiphilicity of the proteins. [30,48] The amphiphilic hydrophobins need to hide their hydrophobic parts from the hydrophilic solvent. At low concentrations of hydrophobin, the proteins dissolve into water as monomers as well as coat the surface of the container they are held in. Above the critical micellar concentration (CMC), aggregates start to form[30] . The class I hydrophobin SC3 is in its monomeric form at concentrations of a few micrograms per milliliter or less. At higher concentrations, starting at 4 μg/mL , the protein is mainly in dimeric form. The class II hydrophobins HFBI and HFBII are similarly monomers in concentrations of a few μg/mL[48]. In increased concentrations, dimers are formed and at higher concentrations, 0.5-10 mg/ml tetramers are in turn formed. Oligomerization is thus increasing with increasing protein concentration. At interfaces the oligomers disassociate and the hydrophobins can rearrange to form surface membranes.[48] Several steps of rearrangement can be involved which results in rodlet structures as described previously. Szilvay *et al.*[49], examined both the hydrophilic and hydrophobic side of a surface membrane or film formed by HFBI in nanometer resolution and found that the film had a highly ordered structure. The authors found that the membrane was highly ordered and had a thickness of only one molecule. The membranes have a very high viscosity. Kisko *et al.*[50,51] used X-ray diffraction and suggested that the membranes have a hexagonal structure with a lattice constant of 5.4 nm. Also, the authors showed that the membranes have a very regular crystalline structure which indicated specific cohesive interactions possibly responsible for the viscosity of the membranes.

1.4.3 Structure

The first chrystallographic structure described of a hydrophobin was that of HFBII by Hakanpää *et al.* [52] The authors here described the three dimensional structure of the protein in a 1 Å resolution and also found that the overall shape of the molecule is globular with a diameter of about 3 nm and a molecular weight of about 7.2kDa. Furthermore, it has a central β structure comprising two β hairpins. Looking at the primary sequence one hairpin is located near the N terminus and the other near the C terminus. The two hairpins connect and interlock and thereby form an anti-parallel β sheet. Between the two hairpins, a α helix is situated which in the tertiary structure lies outside the β barrel. The surface residues of the protein display a large patch formed by hydrophobic aliphatic residues, the hydrophobic patch. This patch is formed mainly by residues situated near the loop regions of the two β hairpins, forms about 12 % of the surface

of the protein and is relatively flat. Furthermore, in other class II hydrophobins the residues forming the patch are conserved and similar residues are found in corresponding positions in sequences of other class II hydrophobins[13]. The protein exposes about half of its hydrophobic aliphatic residues on the surface, forming the patch which is quite unusual as soluble proteins generally form hydrophobic cores in order to stabilize their folded structures. The patch is formed solely by aliphatic residues. For the stabilization of the core, HFBII has an extended network of disulfide bonds. The paired cystein residues described earlier are in the middle of the protein forming double disulfide bonds that are spanning the entire structure.

The crystallographic structure of HFBI is very similar to that of HFBII, consisting of four β-sheets and one α-helix.[52,53] The two hydrophobins also share the same arrangement of disulfide bridges and have a high cystein content. The hydrophobic patch is also conserved between the proteins. HFBI and HFBII further contain exposed hydrophilic side chains which give them the character of an amphiphile. It is likely that all filamentous fungi are secreting hydrophobins[30]. It has also been speculated that class II hydrophobins might have evolved independently from the class I hydrophobins as they have a very low sequence similarity[54]. The low sequence similarity can also be seen between species[4]. The structure of HFBIII is currently unknown but a homology model of HFBIII structure (data not shown) indicates that HFBIII has 4 positively and 5 negatively charged groups on its hydrophilic side.

1.4.4 Surface wetting alterations by using hydrophobins

1.4.4.1 Class I

Wösten *et al.*[14], examined aerial hyphae, typically hydrophobic mycelium, of *S. commune* that express the class I hydrophobin Sc3p. Water droplets placed on the surface of a wild type monokaryon of *S. commune* had contact angles of 115°. The monokaryon mutant of *S. commune* named *thin* does not form aerial hyphae and the water contact angle on the *thin* mutant monokaryon was measured as 40°. Sc3p aggregated on a hydrophilic glass surface produced a surface with a contact angle of 95° and when a solution of Sc3p was allowed to dry down on a the surface of a piece of *thin* mycelium the contact angle was measured as 110° compared to the 40° degrees measured for *thin* monokaryon alone. From these results the authors concluded that the hydrophobicity of aerial hyphae was largely due to self assembled Sc3p.

Lugones *et al.*, have studied the hydrophobic-hydrophilic and hydrophilic-hydrophobic effect on surfaces of the class I hydrophobins ABHI[6] and ABHIII[9] produced by *A. bisporus*. The authors examined hydrophobic-hydrophilic interactions by allowing self assembly of ABHI and ABHIII on Teflon and measuring contact angles. For ABHI, the water contact angle dropped from 100° to 63° for hydrophobin coated Teflon and for ABHIII the uncoated Teflon of 110° water contact angle dropped to 53°. For the examination of hydrophilic-hydrophobic interactions on surfaces by the two hydrophobins, the authors allowed a 0.2 mg/ml solution of ABHI or ABHII on 35 % ethanol to ascend in a filter paper strip in air. During 18 hours, 2 ml solvent was allowed to evaporate after which the paper was dried followed by an extraction of 1 % SDS at at 100° C for 10 min, water wash and final drying. Water contact angle was then used to measure surface hydrophobicity. For ABHI contact angles of 113° and for ABHII the angles were measured 117°. In both cases the paper became hydrophilic just after the evaporation point and the assembled structure of both ABHI and II was shown to form a pattern of parallel 10 nm wide rodlets in these examinations. Using the same techniques described above the class I hydrophobin SC4 of *S. commune*[10] were examined. SC4 was shown to reduce the WCA of the Teflon membrane from 110° to 48° ± 3. After a 1 % SDS wash in 100 for 10 min the WCA was increased to 66° ± 3. When SC4 was allowed to coat paper strips as described above, the after coating WCA was measured as 115° ± 3 after SDS extraction.

Askolin *et al.*[8] used the technique of Lugones *et al.* described previously to examine the hydrophobic-hydrophilic effect on surfaces of the class I hydrophobin SC3 on filter paper and found that SC3 bound over the whole length of the paper strip generating WCAs in the range of 100° - 130°. The WCA of Teflon was shown to be reduced from 109° ± 2 to 40° ± 4.

1.4.4.2 Class II

Askolin *et al.* [8] examined the hydrophilic-hydrophobic properties in the same manner as Lugones *et al.* has done previously and found that HFBI and HFBII reduced the hydrophilicity of filter paper to produce WCAs of 60° – 64° and 60° – 70° respectively. The proteins where here dissolved in water or ethanol in 0.1 mg/ml concentrations. HFBI and HFBII were also examined regarding their abilities to alter the hydrophobicity of a hydrophobic Teflon (WCA 109° ± 2) surface. HFBI and HFBII were incubated overnight in 0.1 mg/ml solution of protein and rinsed with water generated contact angels of 59° ±13 for HFBI and unchanged WCAs for HFBII coating (110° ±2). The layer of HFBI was then shown to be dissolved after boiling with 2 %

SDS. The coating was also shown to be strongly reduced when buffers with salt (pH 3.0, 100 mM NaCl) were used instead of water wash. A mixture of SC3 and HFBI showed that SC3 and HFBI binds simultaneously generating WCAs of 60° ±5 and 72° ±15 where the latter value is measured after treatment with hot SDS. The HFBI is suggested to be dissolving after the SDS wash. de Vries et a.l[7] used the Lugones technique examining the class II hydrophobin CFTH1 from *Claviceps fusiformis*. The water contact angle of Teflon was reduced from 110° to 60° ± 5 after hydrophobin adsorption. The protein layer was not resistant to SDS boiling as was shown on other Class II hydrophobins (HFBI). A filter paper treated with CTFH1 as described previously generated WCA of 105° ± 2.

Wang *et al.*[55] investigated the adsorption of HFB1 (class II) as well as HGF1 (class I) on a hydrophobic surface using 1-hexanethiol by QCM-D, Quartz crystal microbalance with dissipation monitoring. The QCM-D system measures the amount of bound mass as well as the viscoelastic properties of the bound layer by dissipation monitoring. The authors showed that the amount of bound hydrophobin to the surface is pH-dependant. The maximum binding was found slightly above the calculated pI of HFBI, at pI = 5.7. The dissipation values for the adsorbed HFBI surface were shown to be stable which indicates a very rigid layer of HFBI. The authors also investigated the effect of different ionic strengths on the adsorption of HFBI by increasing the concentration of the buffer used. The authors here found that the adsorbed amount of HFBI was not affected by an increase in ionic strength.

HFBI has also been used to change the polarity of a hydrophobic (poly(dimethylsiloxzne)) (PDMS) surface. [56] By submerging sterilized PDMS squares into HFBI solution (100μg/ml in water) for 20 in followed by a blowing off and drying with nitrogen, the polarity was changed. The WCA of native PDMS was 117° and after coating the WCA was lowered to 56,3°.

Li *et al.*[57] used HFBI in order to convert a hydrophobic poly(lactic-co-glycolic acid) (PLGA) film hydrophilic. The WCA of the PLGA before coating was 89.1° and after HFBI adsorption (100μg/ml in water), the WCA was decreased to 47.0°.

1.4.5 Applications

The proposed application areas of hydrophobins are many.[13] Here applications in biotechnology are discussed including potential use in drug delivery, cell- and protein immobilization and as well as biomedical uses coupled to the promising biocompatibility of the proteins.

1.4.5.1 Drug delivery

Valo *et al.*[58] examined the adsorption of HFBII on the lipophilic drug (Beclomethasone dipropionate) in water. The authors found that the precipitation process resulted in three effects; it arrested particle growth, it offered a way to improve stability and the hydrophobin created a layer around the drug that was possible to functionalize. By performing layering studies the fact that the drug particles were covered with hydrophobin was demonstrated. The ability to functionalize the protein by protein engineering enables possibilities for advanced delivery systems or ways to enhance cell wall penetration or localization of the drug, thereby increasing the biovailablity of the drug. Similarly, Scholtmeyer *et al.*[59] used the class I hydrophobin SC3 to coat hydrophobic drugs in aqueous solutions and found that the coating increased the bioavailability of the drugs CyA and nifedipine. Also, the authors found that the pharmacokinetic properties of the CyA was improved after SC3 coating as the peak concentration in the blood was shown to be longer lasting using the hydrophobin coated drug.

1.4.5.2 Biocompatibility and potential use in biomedical applications

The biocompatibility of hydrophobins is an important factor when proposing use in biomedical applications. Examining this, the hydrophobin SC3 and the genetically engineered TrSC3 were added to the medium of 24 h-old fibroblast cultures and it was shown that the assembled hydrophobins were nontoxic to the fibroblasts in amounts up to 125 mg/ml.[60] Furthermore, it has been shown that airborn spores (conidia) of *A. fumigatus* are covered with a surface rodlet layer of the class I hydrophobin RodA and that this layer masks the recognition of the conidia by the human immune system and hence prevents immune response.[3] Hydrophobins thus give excellent indications to good biocompatibility.

SC3 was used to create thin and stable coatings, 10-20 nm thick, by spin coating and adsorption from aqueous solution onto polymeric substrates.[61] Polystyrene (PS) and a copolymer of benzoyl-1,4 phenylene and 1,3-phenylene (PBP) was used. The resulting coated surface was shown to have enhanced lubricity and a reduced surface friction. The friction coefficient was reduced by up to 70 – 80 % compared to PS and 50 – 60 % compared to PBS. This has potential use in coatings for personal care or biomedical applications that requires lubricious, low friction surfaces.

1.4.5.3 Immobilizing cells and proteins

The growth of fibroblasts on Teflon has been shown to be increased by coating the surface with genetically engineered SC3 hydrophobins. [60] The TrSC3 hydrophobin was made by deleting a 25 amino acid long stretch on the N-terminus if the protein or a fusion with RGD has been shown to improve growth of the cells. By allowing HFBI to adsorb on hydrophobic PDMS and as a second step coat the hydrophobin layer with collagen, cell adhesion and growth was promoted whereas the PDMS surface was shown not to promote any cell growth by itself.[56] Neural stem cells (NCS) were allowed to grow on PLGA films modified with a HFBI/serum layer and it was shown that growth was promoted and NCS patterning made possible by using this approach[57].

1.4.5.4 Nanobiotechnology

HFBI has also been shown to be able to efficiently dissolve single walled carbon nanotubes (SWNT) in water. [62] By adding HFBI in aqueous solution in concentration as low as 0.25 mg/ml to 50μg/ml SWNT followed by ultrasonication and centrifugation, HFBI was proved to be an extremely capable solubilizing agent for SWNTs. HFBI was also labeled with 1.4 nm gold nanoparticles allowing for effective monitoring of the binding of hydrophobin to SWNTs by electron microscopy.

Laaksonen *et al.*[63]used HFBI to create a one-step method for the exfoliation and functionalization of graphene. A water dispersible suspension of protein coated flakes of graphene as well as ultra thin flakes of graphite can be attained by the method. The hydrophobic patch attaches to the graphite surface resulting in the protein covered flakes. This results in the possibility to add a specified functionality to the part of the protein that does not bind to the surface. By labeling the HFBI with gold nanoparticles, the authors showed that this kind of functionalization is possible, making e.g. the development of biosensors promising from this approach.

1.5 Aims of study

The amphiphilic nature and the binding abilities of three class II hydrophobins, HFBI, HFBII and HFBIII are examined in this work by allowing the proteins to bind to polar surfaces in submerged conditions, replicating the role hydrophobins have when forming hydrophobic surface coatings by self assembly on fungal spores and mycelia of filamentous fungi.

The adsorption on the solid polar hydrophilic surfaces is aimed to have the hydrophobins bind so that the hydrophobic face of the protein would turn outwards rendering the polar surface hydrophobic via charge-charge interactions mainly. Surfaces used include SAM layers as well as well as a spin coated polymer surfaces. The hydrophobicity of the layer is measured with contact angle measurements and the amount of bound mass is examined by quartz crystal micro balance, QCM-D. Furthermore, the variability of the binding is examined with aspect on the influence of ion interactions of mono- and multivalent ions. For complementary experiments hydrophobin adsorption on a hydrophobic and a negatively charged surface as well as Resonance Enhanced Surface Impedance technology (RESI) is carried out.

2 Materials and Methods

2.1 Reagents and chemicals:

HFBI, HFBII and HFBIII, was purified from *T. reesei* mycelium and purified by reversed phase chromatography as described earlier. [64,65]

The buffers used for adsorption experiments at different pHs were 10 mM sodium acetate-acetic acid (pH 4.0, 5.0), sodium phosphate monobasic- sodium phosphate dibasic (pH 6.0, 7.0), Tris-HCl (pH 8.0) and glycine-NaOH (pH 9.0, 9.5, 10.5) were used. For ionic strength experiments the following buffers were used: 10 mM: borax-boric acid (pH 8.9; 10 to 500mM NaCl) For hydrophobin adsorption on gold coated quartz chips the buffers were 10 mM borax-boric acid (pH 7,5-8,8) and glycine-NaOH (pH 8,6-9,9) In the SEC, 50 mM sodium acetate-acetic acid (pH 4.0, 5.0, 200 mM NaCl) and 50 mM glycine-NaOH (pH 9.0, 200mM NaCl) were used.

2.2 Preparation of SAM layers

Self- assembled monolayers (SAMs) were prepared to form cationic, anionic and non-polar aliphatic surfaces. A SAM is a highly ordered, one molecule thick film that is formed on a solid support, here on gold. Typically, molecules that forms SAMs have one group that binds to a substrate, a chain in the middle allowing tight packing by van der Waals forces, and a head group that gives the formed SAM desired properties such as charge, hydrophobicity or biospecificity. Gold is the mostly used substrate but e.g. silver, copper, platimum or palladium can be used. After immersing the substrate in ethanolic solution of the thiol, a disordered SAM is formed within seconds. Soaking at least 12 hours generates more ordered and crystalline SAMs and the layer is ready for use. [66 67]

Here, for preparing cationic surfaces N,N,N-trimethyl-(11-mercaptoundecyl)ammonium chloride (HS(CH2)11NMe3+Cl-) thiol (TMA) (Prochimia Surfaces, Poland) was used, for hydrophobic surfaces 1-hexanethiol ($CH_3(CH_2)_5SH$) (HEX) (Sigma-Aldrich, USA) was used, and for anionic surfaces 11-mercaptoundecanoic acid (MUA) (Sigma-Aldrich) was used. The SAM coatings were prepared either on gold coated quartz crystal microbalance with dissipation monitoring (QCM-D) sensor disks (QCX 301, Q-Sense AB, Sweden) or on gold coated glass disks (with a chromium adhesion layer) (Bionavis, Finland).The coating of the sensor discs was performed as

follows: The discs where cleaned in a UV/ozone chamber (Procleaner, Bioforce) for 10 minutes followed by a 10 minute heating in a 75 °C $H_2O/NH_3/H_2O_2$ mixture (5:1:1). The sensor disks where then cleaned thoroughly with Milli-Q (Millipore) followed by a second UV/ozone cleaning. The discs where then immersed overnight in room temperature in a 10 mM HS(CH2)11NMe3+Cl-/ethanol solution for hydrophilic SAM formation and a 50 mM HEX/ethanol solution for hydrophobic SAM formation as well as 50 mM MUA/ethanol for the anionic SAM. Before use the thiol coated sensors were cleaned with pure ethanol and Milli-Q and dried with N2 (g).

Preparation on PEI surfaces: For the forming of anionic, hydrophilic SAM surfaces, Polyethyleimine (PEI) (Sigma-Aldrich) was spin coated on SiO_2 QCM-D sensor discs (QSX 303, Q-Sense AB, Sweden) to create a positively charged polymer surface. The discs where spin coated in atmospheric pressure with a 40 ul drop of 1g/l PEI in MQ for 90 sec in 3000 rpm and cleaned with MQ with cotton tops on the sensor parts of the discs.

2.3 Hydrophobin adsorption using QCM-D

Quartz crystal microbalance with dissipation monitoring, QCM-D, was used to measure frequency and dissipation simultaneously and to thereby calculate the Sauerbrey mass of the bound protein layer measured (D4-QCM system, Q-Sense AB, Sweden). The QCM-D system measures the amount of bound mass as well as the viscoelastic properties of the bound layer by dissipation monitoring. The adsorbed mass per areal unit was calculated from the resonance frequency changes using the Sauerbrey relation, $\Delta m = -C\Delta f/n$, where Δm is adsorbed mass, Δf is frequency change, C = 17.7 ng·Hz·cm^{-2}, and using the third overtone (n = 3). The dissipation change in the experiments was typically < 0.2. HFBI, HFBII, and HFBIII were used in a 0,1 mg/ml solution, based on the buffer used at each measurement. HFBI, HFBII and HFBIII, 300 µL respectively, was pumped through each measuring chamber with a flow rate of 100 µL/min. The sensors were left to stabilize after adsorption for 30-80 minutes in order to attain a stable baseline of the resonance frequencies and were then washed with the same buffer used for dilution until a stable baseline was attained anew.

2.4 Hydrophobin adsorption on gold coated quartz chips

Gold coated chromium based quartz chips (Bionavis, Finland) were used to measure contact angles of adsorbed hydrophobin with a narrow pH range. The chips were cleaned and coated with a SAM in the same manner as QCM sensor chips as described previously. Coating with hydrophobin was carried out in a plastic 6 well Petri dish. HFBI was used in a 0.1 mg/ml solution, based on the buffer used at each measurement and a total of 1.5 ml of solution was contained in each well during adsorption of hydrophobin. The chips were left to stabilize after adsorption for about 45 minutes before washing. During washing, the excess hydrophobin solution was removed from the wells with a disposable pipette followed by a soaking of the chips immersed in 150 ml of respective buffer used in the experiments in a glass beaker for about 10 min. The chips were then washed thoroughly in MQ water before being dried with N_2 (g).

2.5 Water contact angle

Water contact angle (WCA) measurements were measured with a CAM 200 equipment (KVS Instruments, Biolin AB, Sweden) was used where a 6 µl drop of MQ water (Millipore) was put on the surface of choice (SAM or hydrophobin coated SAM) and a series of 15 pictures were taken with a 5 second interval from which the average contact angle could be calculated. The WCA was measured before and after each protein adsorption experiment. The reported WCA values were determined as the average of three measurements.

2.6 Hysteresis

Hysteresis measurements were carried out on a TMA SAM disk with adsorbed HFBI at pH 9. In order to determine the hysteresis of the surface, a 4 µl drop was first applied to using the thin needle of the CAM 200 dispenser. The needle was then lowered into the drop closer to the surface/drop interface at the bottom. In order to measure the advancing CA, a 6 µl drop was added to the drop at the speed of 0.1 µl/s. At points just before the stable three phase line was moving, the maximum advancing CA was measured. For measuring the receding CA, water was withdrawn at the same speed as filling until all water is removed, a total of 10 µl. At the point where the three phase line starts to move, the receding contact angle is measured. The average difference between the advancing and receding drop of three drops per surface gives the hysteresis value.

2.7 Size exclusion chromatography

Size exclusion chromatography of HFBI was carried out as described earlier by Szilvay *et al.*[48] Hydrophobin samples, 100 mM in 50 mM buffers as seen in reagents and chemicals, were injected (100 μL) into a Superdex 75 column (Amersham, Sweden) using an Äkta Explorer (GE Healthcare, U.S.A) chromatography system. Sample elution was detected with UV absorbance at 230 nm.

2.8 Surface characterization by impedance measurements

For impedance measurements, the micro impedance based instruments, z-LAB (Layerlab AB, Sweden) was used. The z-lab is based on Resonance Enhanced Surface Impedance technology (RESI) and is here used to monitor changes in impedance in order to distinguish between loose and dense layers as well as the insulating properties of a protein layer. Gold coated ZO-PADS sensors were provided by Layerlab and used in all experiments. The sensors were coated with SAMs as described above. HFBI was used in a 0,1 mg/ml solution dissolved in 50 mM glycine-NaOH buffer pH 8.85. 75 µL of dissolved HFBI was pumped through the measuring chamber over the sensor at a flow rate of 25 µL/min for 3 min. The sensors were then left to stabilize for 10-30 min in order to attain a stable base line in terms of impedance. The sensors were then washed with the same buffer used for dilution at 25 µL/min until a stable baseline was attained anew. The capacitance of the protein layer, $C_{Protein}$, is calculated from the SAM capacitance, C_{SAM} which is measured just before protein injection, and the total capacitance, C_{Total}, which is measured after wash, using the following formula: $C_{Protein} = 1 / ((1/ C_{Total}) - (1/ C_{SAM}))$

3 Results

3.1 Adsorption of hydrophobins on surfaces

Adsorption curves of a QCM-D sensogram displaying Sauerbrey mass is shown in Figure 3 where the adsorption of HFBI on SAM surfaces of TMA at pH 9.5, HEX at pH 9.0 and MUA at pH 9.0 respectively is shown as a representative example of hydrophobin adsorption. The WCA was measured on all QCM-D chips before and after each QCM-D adsorption experiment. In an adsorption experiment, hydrophobin is added and the adsorbed mass is increasing until a maximum amount is reached. After this, the adsorbed hydrophobin is allowed to bind and settle before the buffer wash is started to remove any loosely bound proteins.

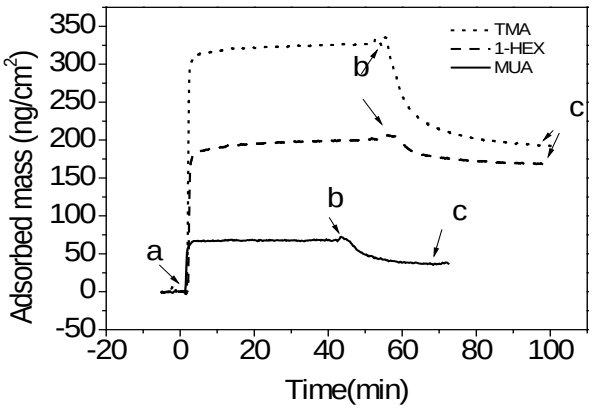

Figure 3 QCM-D sensograms showing representative curves of HFBI binding to different SAM surfaces. The surfaces used were hydrophobic HEX (at pH 9.5), anionic MUA (at pH 9.0) and cationic TMA (at pH 9.0). (a) Corresponds to hydrophobin injection, (b) to buffer wash and (c) to end of buffer wash where adsorbed mass and WCA was measured. The adsorbed mass was calculated using the Sauerbrey relation as described in Materials and Methods.

3.1.1 Hydrophobic surfaces

The adsorption of HFBI and HFBII on a hydrophobic HEX SAM surface was measured over a pH range between 4.0 and 10.6 using QCM-D. Corresponding water contact angles were measured on the same surface at a subsequent experiment. For HFBI, the measured values of adsorbed mass on the HEX SAM surface were between 170 and 282 ng/cm^2 depending on pH (Figure 4 A). For HFBII, the amount of adsorbed mass shows a similar pattern as that of HFBI with values of adsorbed mass between 188 and 270 ng/cm^2. The adsorption reached maximum levels within minutes after hydrophobin injection. Buffer wash typically removed only about 10

% of the adsorbed protein (Figure 3). The dissipation change in the experiments was typically below 0.2 indicating a rigid layer (data not shown). WCAs were measured before and after each QCM-D adsorption experiment. The WCA of a freshly prepared HEX SAM was 92.0 ± 6.3° before deposition. After protein adsorption the surfaces were clearly more hydrophilic with WCA values between 39° and 56°, and between 38° and 50°, for HFBI and HFBII, respectively (Figure 4 B).

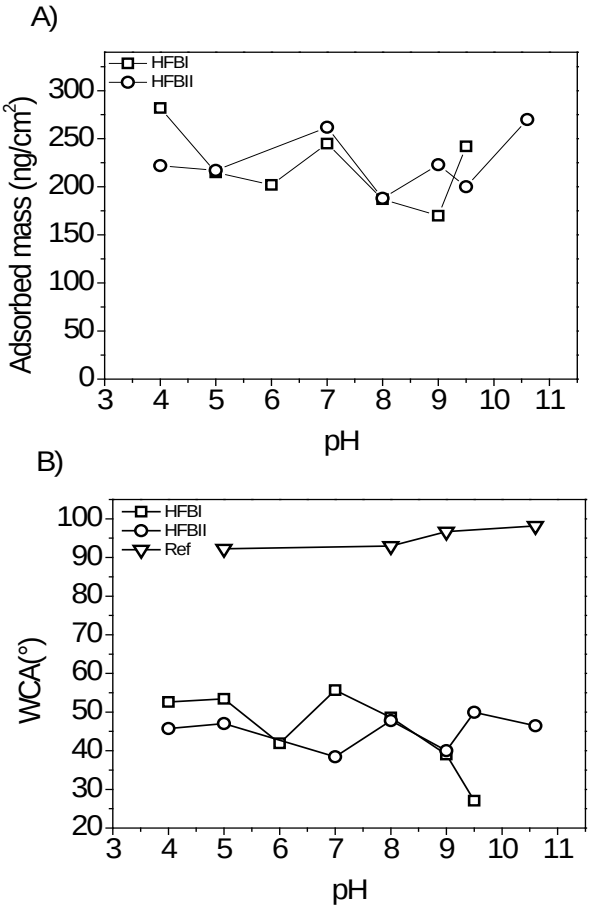

Figure 4 Adsorption of hydrophobins on hydrophobic surfaces. (A) Adsorbed mass of HFBI and HFBII on hydrophobic HEX SAM as a function of pH as observed by QCM-D. (B) WCAs of the same surfaces after adsorption of HFBI or HFBII in QCM-D runs as a function of pH. A negative control surface (labeled Ref) treated similarly but without addition of protein is also shown.

3.1.2 Cationic surfaces

The binding of HFBI, HFBII and HFBIII on two types of cationic surfaces was measured; cationic trimethyl amine (TMA) SAM and spin coating cationic polymer polyethyleneimine (PEI).

The protein adsorption to cationic TMA SAM surface was measured over a pH range between 4.0 and 10.5 as shown in Figure 5 A. The corresponding WCAs were measured on QCM-D sensors before and after protein adsorption, and are shown in Figure 5 B. Before deposition the TMA SAM had a WCA of about 22.3° (± 5.7°). For hydrophobin adsorbing on a TMA SAM, close to half of the initially bound mass was typically removed from the surface during the wash step (Figure 3). This indicates an initial, less tightly bound double layer being washed off to form a more rigid single layer after wash. Also, dissipation changes were below 0.2 in all experiments indicating a rigid layer. For HFBI, the maximum of adsorbed mass is found at pH 9.0 where the adsorbed mass of 215 ng/cm2 is measured. This can be described as equivalent with a monolayer as the Sauerbrey mass of hydrophobin adsorbed on a QCM sensor is estimated by to about 200 ng/cm2. HFBII shows a general lower amount of bound mass compared to HFBI. The highest amount of adsorbed mass is found at pH 10.5 as79 ng/cm^2. HFBIII shows a similar behavior of bound mass as that of HFBII. At pH 5.0 the highest value of mass is measured; 126 ng/cm^2.

All three proteins show a similar curvature of WCA as a function of pH with a lower peak at pH 4.0 – 5.0 and a higher, maximum WCA peak at pH 8.0 – 9.0 (Figure 5 B). At the first lower peak of WCA for all three hydrophobins the reference curve displays a similar curvature. However, at the second peak situated around pH 8.0 – 9.0, the reference graph does not show elevated WCA values whereas the hydrophobin coated samples show contact angle values around 60° – 70°. This peak is thus generated by hydrophobin adsorption and following increase of WCA. HFBI has a maximum value of WCA of 62.6 ° at pH 9.0, HFBII a maximum of 69.0° at pH 8.0 and HFBIII a maximum of 61.9° at pH 8.0. CAM pictures of the drops corresponding to pHs with the highest average contact angle for each protein are shown in Figure 5 D.

In order to further examine the pH dependency of hydrophobin adsorption and hydrophobization of cationic surfaces, HFBI was allowed to adsorb on SAMs formed on gold coated quartz chips

at a narrow pH range (Figure 5 C). A pH range of 7.5 – 9.9 using 10 mM borax-boric acid (pH 7.5-8.8) and glycine-NaOH (pH 8.6 – 9.9) buffers in room temperature was used and the WCA as a function of pH shows a clear trend in the range. For the borax buffer, the WCA is lower at high and low pHs and has a maximum at pH 8.2 – 8.4 with 62.7 and 62.2° WCA respectively. There are variations between the two buffers and at higher pHs of the glycine buffer experiments, the WCA values are showing a greater spread (roughly 5°). Some of this spread is due to experimental variation, but a buffer component caused effect cannot be ruled out. Also, at these pHs the charge of the surface is more neutral than positive as the pKa of TMA is 9.81.

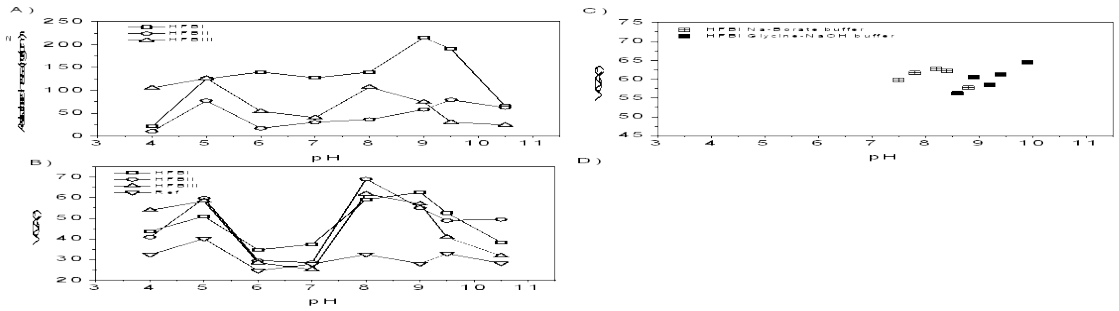

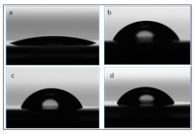

Figure 5 Adsorption of hydrophobins on cationic SAM surfaces. (A) QCM-D derived adsorbed mass of HFBI, HFBII and HFBIII on TMA SAM surface as a function of pH. (B) WCAs of the same surfaces after hydrophobin adsorption in QCM-D runs as a function of pH. WCAs after HFBI, HFBII or HFBIII adsorption are shown, as well as a negative control surface (labeled Ref) that was treated similarly but without addition of protein. (C) QCM-D derived adsorbed mass of HFBI, HFBII and HFBIII on TMA SAM at a narrow pH range. (D) Water drop profile shapes from WCA measurements on TMA SAM surfaces. Drop before protein coating is shown at (a) as well as drops after HFBI (at pH 9.0) (b), HFBII (at pH 8.0) (c), and HFBIII (at pH 8.0) (d) coating. The obtained WCAs were 22.3° before deposition, and 62.6°, 69.0°, and 61.9°, after HFBI, HFBII, and HFBIII adsorption, respectively.

3.1.2.1 Cationic PEI surfaces

A third set of experiments was conducted in order to study the effect of the underlying charged surface on the assembly of hydrophobins. QCM experiments using SiO_2 sensors spin coated with Polyethyleneimine (PEI) in order to create a polymeric, positively charged surface were performed at the pH range 4.0 – 10.0. The amount of adsorbed mass as a function of pH can be seen in Figure 6 A and the corresponding WCAs are shown in Figure 6 B. The spin coated PEI surface had a WCA below 10° before deposition. The amount of adsorbed mass as a function of pH shows a first peak at pH 5.0 where 150 ng/cm^2 of adsorbed HFBI is measured. A maximum value of mass is measured at pH 10 as 260 ng/cm^2. The adsorption of HFBI on the PEI surface generates two peaks of WCA as a function of pH, a first peak is measured at pH 5.0 generating a WCA of 30.3° and a second, maximum peak is found at pH 8.0 where WCA of 50.3° is found.

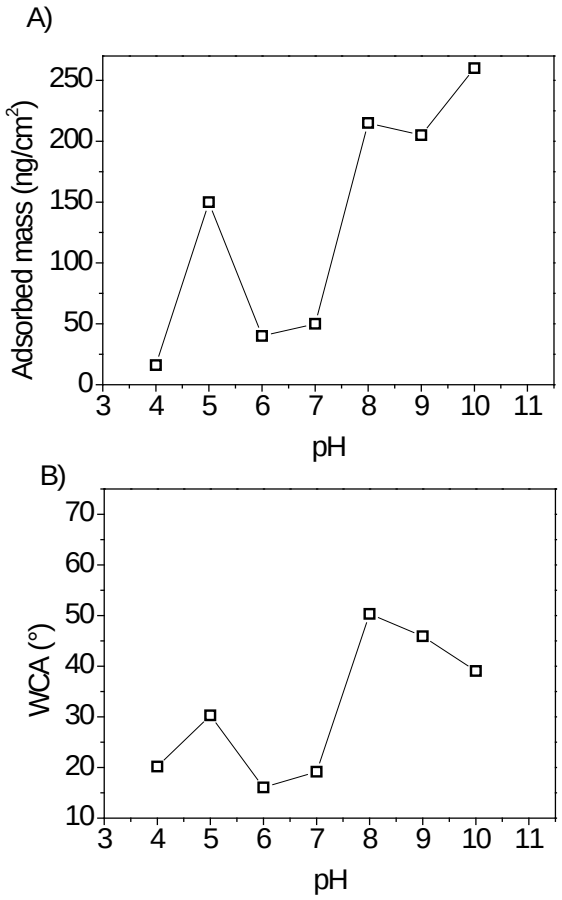

Figure 6 Adsorption of HFBI on cationic PEI surfaces. (A) Mass of adsorbed HFBI on cationic PEI surface as observed by QCM-D as a function of pH. (B) WCAs of the same surfaces after adsorption of HFBI in QCM-D runs as a function of pH. The WCA of PEI surface before deposition was < 10°.

3.1.3 Anionic surfaces

The adsorption of hydrophobins on anionic surfaces was examined by allowing HFBI to adsorb on the highly hydrophilic, anionic surface of 11-mercaptoundecanoic acid (MUA) in a QCM-D experiment. A negative control without protein adsorption (buffer only) was also conducted on this surface. Before deposition the MUA SAM had a WCA of about 31.5° (± 3.3°). Adsorption of hydrophobin on the anionic SAM displays a similar effect as that of the hydrophobic SAM surface of a more tightly bound layer which at pH 9.0 however is low in terms of bound mass (Figure 3). The adsorption was measured over a pH range between 4.0 and 10.5. The maximum value of adsorbed mass, 185 ng/cm^2, is measured at pH 5.0. (Figure 7 A) The corresponding WCAs of the MUA SAM surfaces with adsorbed HFBI are low overall and vary between 17.8° and 34.6° with the highest measured WCA measured at pH 5.0 (Figure 7 B). The adsorption of hydrophobin is thus slightly lowering the contact angle of the hydrophilic MUA surface. Values of MUA SAM negative control also generate slightly lower values of WCA. These results show that HFBI interactions with anionic surfaces are very different from interactions with cationic surfaces.

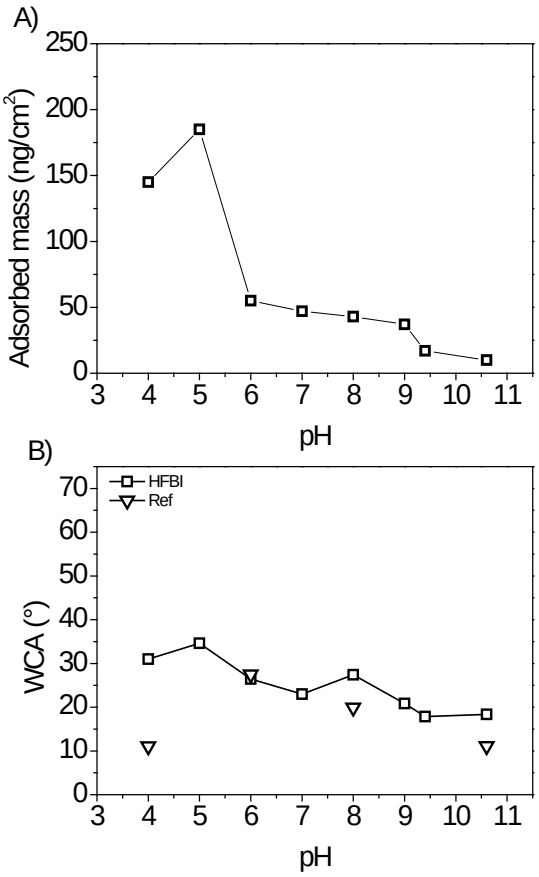

Figure 7 Adsorption of HFBI on anionic MUA SAM. (A) QCM-D derived mass of adsorbed HFBI on MUA as a function of pH. (B) WCAs of the same surface after HFBI adsorption as a function of pH as well as a negative control surface (labeled Ref) that was treated similarly but without addition of protein.

3.1.4 Effect of ionic strength on HFBI binding to TMA SAMs

Increasing ionic strength and its influence on the adsorption of hydrophobin was examined using cationic TMA SAM surfaces. Binding was studied following both QCM-D and WCA. In the QCM-D experiments HFBI and a 10 mM glycine pH 9.0 buffer with NaCl in different concentrations (0, 10, 25, 50, 75, 100, 500 mM) were used. The salt caused a reduction in adsorbed mass in all cases (Figure 8). From the Initial value of 215 ng/cm^2 for 0 mM NaCl, the amount of adsorbed mass was decreased to 175 ng/cm^2 already at 10 mM salt and continues to decrease over the salt gradient to about 50 ng/cm^2 for 100 and 500 mM Nacl concentration. Also, the WCA was shown to be decreasing by increased NaCl concentration. The Initial WCA of 62.6° was lowered to 45.5° already at 10 mM NaCl.

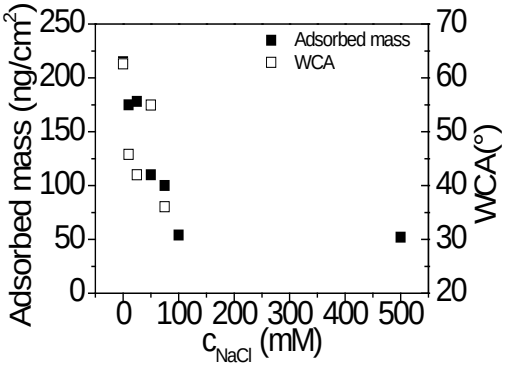

Figure 8 HFBI adsorption to cationic TMA SAMs as a function of NaCl concentration, performed at pH 9.0. QCM-D derived adsorbed mass and WCA are shown.

3.2 Characterization by capacitance measurements

The capacitance of the adsorbed hydrophobin layer was measured for both TMA and HEX SAMs at pH 8.9. HFBI binding to HEX SAM generates $C_{Protein}$ values with an average of 4.97 ± 0.8 µF/cm^2 whereas binding of HFBI to TMA SAM results in considerably higher $C_{Protein}$ values averaging at 73.70 ± 29.3 µF/cm^2. The much lower capacitance value on the layer formed on the hydrophobic HEX surface compared to the cationic surface indicates the HFBI binding on the hydrophobic surface results in a much denser and insulating layer whereas the binding to the cationic surface results in a surface which is less insulating and possibly less structured. The

capacitance of the underlying HEX thiol layer generates average c-values between 2.16 and 2.63 $\mu F/cm^2$ whereas the charged and more bulky TMA SAM generates an average capacitance values between 4.66 and 4.94. (Figure 9)

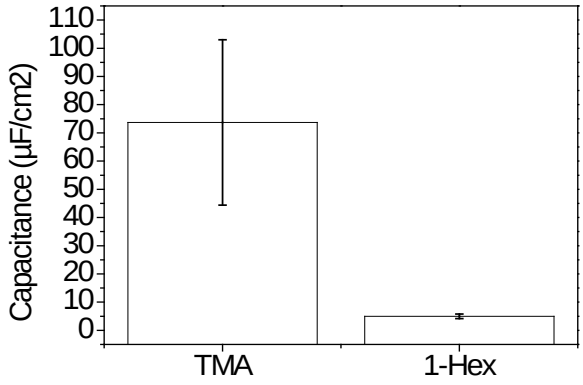

Figure 9 Capacitance for HFBI adsorbing on SAM layers formed by TMA or HEX at pH 8.9.

3.3 Size exclusion chromatography

Size exclusion chromatography was performed with 50 mM buffers and 200 mM NaCl at pHs 4.0, 5.0, and 9.0 with HFBI (100 μM) on a TMA SAM surface. Data is shown in Figure 10. The protein does not denature or change its conformation in the pH range.

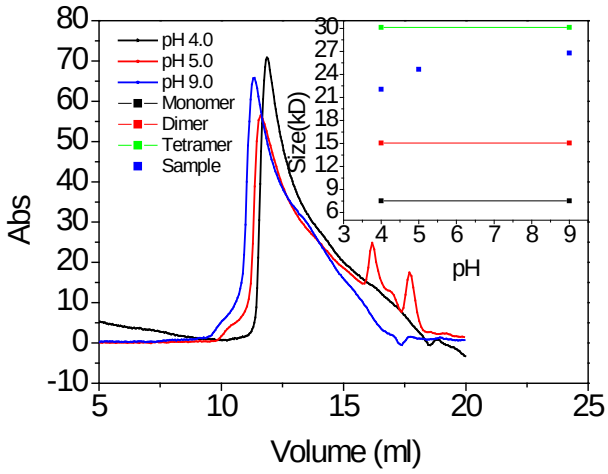

Figure 10 Size exclusion chromatography. Experiments were performed with 50 mM buffers with 200 mM NaCl at pHs 4.0, 5.0, and 9.0 with HFBI on a TMA SAM surface

3.4 Hysteresis

Hysteresis measurements were carried out on a TMA SAM disk with adsorbed HFBI at pH 9.0. The average advancing CA was 62.5° and the average receding 15.0° rendering a hysteresis value of 47.4°.

4 Discussion

In this thesis it is shown that class II hydrophobins can bind on to submerged polar surfaces and thereby increase the hydrophobicity of the surface. This binding is highly dependent on pH and the charge of the underlying surface. The goal of replicating the role of hydrophobins when forming hydrophobic surface coatings by self assembly on fungal spores and mycelia of filamentous fungi has thus been reached and is discussed in detail below.

On cationic surfaces the adsorption of hydrophobin to the TMA SAM results in the most elevated contact angels. HFBI has an average WCA of 62.6° at pH 9.0, HFBII as average of 69.0° at pH 8.0 and HFBIII has an average WCA of 61.9 ° at pH 8.0. The binding of the hydrophobins to the positively charged TMA is also shown here to be pH dependant and is reduced to low levels by increased NaCl concentrations. Following this, the binding in cationic surfaces is proposed to be due to local charge-charge interactions and as a result, the local charges on the surface of the protein are of greater interest than the overall pI of the protein. The charged residues opposite of the hydrophobic patch of the amphiphilic proteins are thought to interact with the solid polar surface in such a way as the hydrophobic patch is turned outwards against the solution resulting in a hydrophobic surface coating (Figure 11 A). Hysteresis experiments results in a high value, 47.4°, showing that the surface formed is rough. This value is however more of interest regarding superhydrophobic surfaces. Furthermore, adsorption of HFBI on a positively charged PEI surface generates elevated WCA with the highest measured average angle of 50.3° at pH 8.0. HFBI adsorbs on a positively charged PEI surface at higher pHs in amounts that corresponds to a monolayer. The WCAs are elevated up to 50.3 ° at pH 8. Charge density and roughness of the surface is likely to cause the result of slightly lower WCA compared to the smooth TMA SAM surface. Nevertheless, the class II hydrophobin HFBI has here been shown to adsorb on, and make two different positively charged hydrophilic surfaces hydrophobic. The pH dependency of the proteins on the PEI surface strongly resembles that of the TMA but is lower overall. The peak around pH 8 – 9 is the true peak, peak at pH 5 – 4 buffer generated. The TMA and PEI can be seen as two replicates for binding to a cationic surface. HFBII displays the highest WCA of the proteins, which can be linked to its role in forming hydrophobic coatings on spores. On TMA, Higher amounts of bound mass found is for HFBI

(monolayer at pH 9.0) compared to HFBII and HFBIII, showing that a monolayer is not necessary for elevated WCAs. The fact that the proteins can render similar WCAs in different pHs whereas the amount of mass is varying indicates that the structural organization of the surface is likely to be important for the hydrophobic properties of the formed layers.

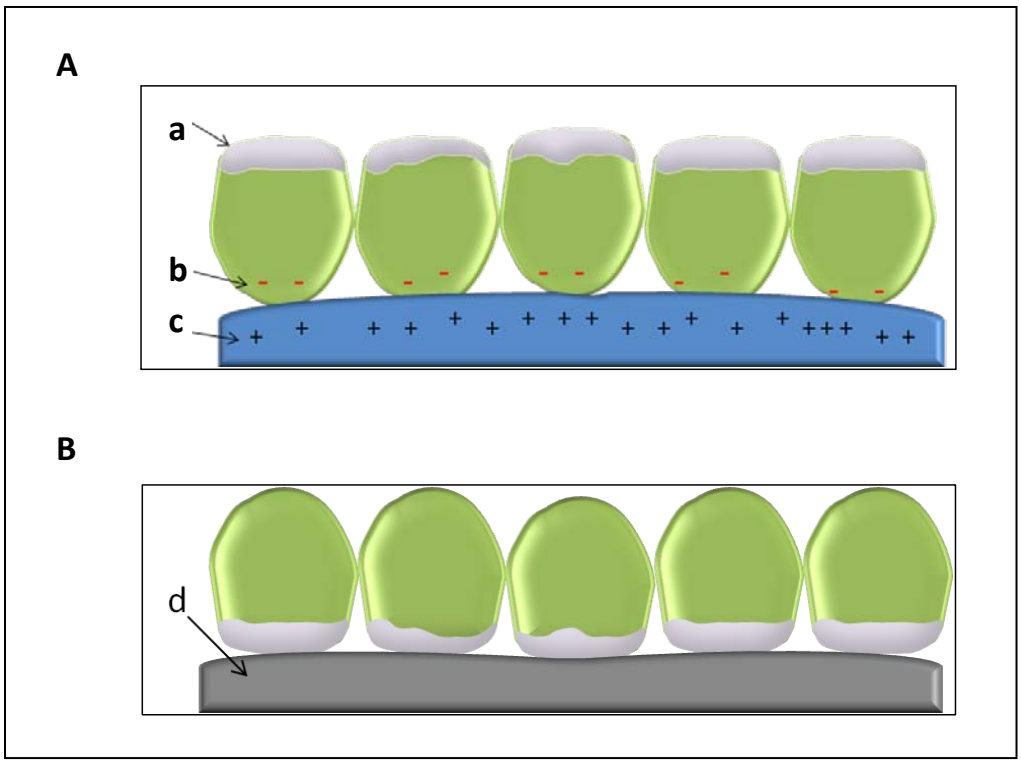

Figure 11 Schematic presentation of a proposed model of adsorption of hydrophobin to cationic and hydrophobic surfaces. (A) Interaction to a cationic surface. The hydrophobic patch (a) of the hydrophobin forms a hydrophobic outer layer as negatively charged residues (b) opposite of the hydrophobic patch of the amphiphilic proteins are interacting with the positive charges (c) of the solid cationic surface in such a way that the hydrophobic patch is turned outwards against the solution resulting in a hydrophobic surface coating. (B) Interaction to a hydrophobic surface. The hydrophobic patch is adsorbing via hydrophobic interactions to the hydrophobic surface (d) rendering the hydrophilic side of the protein outwards.

Hydrophobin binding on anionic MUA slightly lowers the starting WCA and binds low mass. This is indicating areas of low binding formed by hydrophobic interactions between patch – surface. The protein is thus not adsorbing to any greater extent with the hydrophobic patch facing the medium which would have generated elevated WCAs as seen with TMA and PEI. This indicates that the positively charged residues on the hydrophilic side of the protein are not likely to interact with the negative charges of the surface.

Hydrophobins adsorbing on hydrophobic HEX SAM results in lowered WCA and the mass and WCA is stable over the pH range around levels of a monolayer. As a result, hydrophobic interactions between the surface and the hydrophobic patch is claimed as causing binding here (Figure 11 B). The results confirms the experiments performed by Wang *et al.*[55], who showed that HFBI forms a rigid monomolecular layer on a HEX SAM where the hydrophilic side is exposed towards the surroundings. The authors here further showed that the exposed side could bind other proteins to this side while being bound as a monolayer to the hydrophobic surface. This binding was however pH dependant and charge-charge interactions where suggested as responsible for the binding. The ion exchange properties of the hydrophilic side of the protein has in this work been shown to work as the results of Wang *et al.* suggested, by charge-charge interactions. A layer of hydrophobin bound on HEX SAM does not wash off to any greater extent whereas a layer adsorbed on TMA or PEI shows a clear washing off effect. This is believed to be caused by a possible primary lightly bound double layer that is being washed off with running buffer to leave a stable monolayer form.

Charged residues: Local charges are of greater interest than pI when binding to charged surfaces as the charges are situated at specific orientations on the hydrophilic side of the protein. The differences in charged residues are believed to explain the differences in bound mass between the proteins. MUA results indicate that negative surface-positive residues interactions are not likely. The number of charged residues is not essential as HFBII has a higher amount of charged residues than HFBI (Figure 12) but binds less amount of protein. The shielding of neighboring residues of opposite charge as well as the overall availability of the residue is likely of greater importance. HFBI displays a large area of negative charge formed by two aspartates in close proximity on the hydrophilic part of its surface, opposite to the hydrophobic patch. In this large negative area the protein is able to bind strongly to the positively charged surface by charge-charge ineractions. However, HFBI also displays an Arg and Lys in proximity to this negative site with pKas of 12.1 and 10.67 respectively. At lower pHs, the residues are of positive charge and chould then act as repelling towards a positive surface. A TMA surface has a pKa of 9.81 and closer to pH 9.81 the Arg and Lys are less positive and thus less staring and over 9.81 the surface is neutral. This could explain the increase in mass of HFBI up to around pH 9 which is in turn decreasing in higher pHs. The staring effect of the positively charged residues is decreasing

as the become more and more neutral closer to their pIs while the surface is still positive up to pH 9.81 and the negative site can bind more and more undisturbed. HFBII displays a smaller surface of negative charge on its hydrophilic side and also binds lower amounts of mass on the TMA surface compared to HFBI. The positively charged and thus staring His (pKa 6.04) is neutral above pH 6.04 and is thus not staring- HFBII can increase binding as the single Asp is continuously negatively charged and binding to a surface that is positive up till pH 9.81, where the surface is neutral and binding decreases. Regarding the positively charged PEI surface, the pKa is likely high and the surface is positive over the whole range. Following the same ideas as for TMA, the decreasing positive charge of the arg and lys increases binding at higher pHs without any drop when the negative site is allowed to bind with reduced staring effect to a continuingly positive surface.

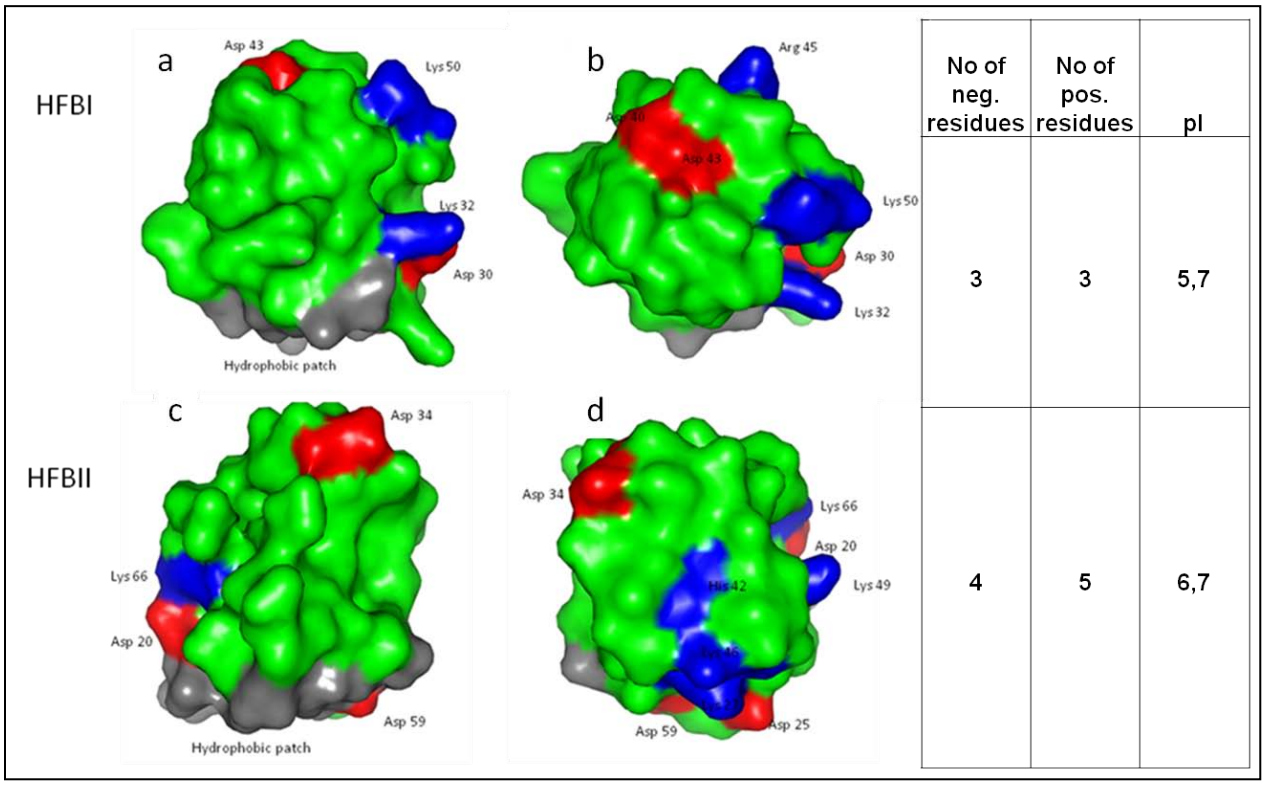

No of neg. residues	No of pos. residues	pI
3	3	5,7
4	5	6,7

Figure 12 Structure of HFBI and HFBII. (a) or (c) shows the protein with the hydrophobic patch (grey) at the bottom and (b) or (d) as a top view of a or c. The Ionizable side chains are shown where red is negative and blue is positive charge in neutral pH. Number of charged residues and pI of the proteins are also shown in the figure. The molecular structure of HFBIII, also used in this study, is currently unknown. Homology models suggest a similar structure to HFBI and HFBII.

In the size exclusion chromatography experiments the protein did not denature or change its conformation in the conditions examined. From this it can be assumed that the hydrophobin is

displaying the charged residues in the same way in the whole pH range and that the negatively charged aspartate residues can be used in order to explain the binding to the positively charged surface. In The QCM-D experiments, the dissipation was kept at a constant level at all conditions which would imply a rigid layer of hydrophobin bound to the surface. (Data not shown). However, hydrophobin form a less insulating layer on TMA than HEX according to RESI experiments. The layer can thus be seen as rigid but poorly insulating. The RESI results are confirming the results from QCM and WCA that the proteins are binding differently to the two SAMs formed by HEX and TMA. The hydrophobic patch is believed to bind to the on HEX SAM and to be the opposite way on the TMA SAM. The hydrophobic interactions between the hydrophilic HEX SAM and the hydrophobic patch of the protein can be seen as more effective at filling up gaps and creating an insulating protein layer with a low capacitance following the RESI results. The TMA- HFBI layer is less effective in gap filling as a result of it being formed by charge- charge interactions and is less insulating and therefore displays higher capacitance values.

5 Conclusions

This thesis examines the ability of hydrophobins to self assemble and form membranes on solid polar surfaces in submerged conditions, replicating the role of hydrophobins when forming hydrophobic surface coatings by self assembly on fungal spores and mycelia of filamentous fungi. It shown that class II hydrophobins can bind on to submerged polar surfaces and thereby increase the hydrophobicity of the surface. This binding is highly dependent on pH and the charge of the underlying surface. The largest increase in WCA was found on cationic TMA SAM surfaces where the WCA of 69.0° at pH 8.0 is measured after coating with HFBII. It is expected that the proteins are exposing their hydrophobic sides towards the solution and are binding via charge-charge interactions to the polar surface in a binding that is pH dependant. Previously, hydrophobin membranes where the hydrophobic sides are exposed has been performed by allowing the membrane to form at the air-water interface and then as a second step attach it to a polar support[6-11]. Membranes formed in this way have been allowed to dry or ascend on polar surfaces such as filter paper. However, pre-organization at the air water interface followed by an ascending step is an unlikely explanation for how hydrophobins assemble in nature for example on spores and hyphae and the results shown here are concluded as replicating this more closely.

The formation of molecular membranes on various interfaces is a very important biological function of hydrophobins and also for many technical applications such as biosensors and medical implants. As hydrophobins have received large attention as industrially useful proteins[13], the knowledge derived from this thesis show great potential to result in new inventions and applications.

Acknowledgements

I would like to thank Prof. Markus Linder for giving me the opportunity to work as master student in his group and also for excellent support and help. I would also like to sincerely thank Dr. Géza Szilvay for his advice and continuous support which has been of great help throughout the work with this thesis. Dr Michael Lienemann and the rest of the members of the group Nanobiomaterials at VTT are all thanked for their kind help and support. Riitta Suihkonen is thanked for technical assistance.

References

(1) Wösten, H. A.; van Wetter, M. A.; Lugones, L. G.; van der Mei, H. C.; Busscher, H. J.; Wessels, J. G. *Curr Biol* **1999**, *9*, 85.

(2) Nakari-Setala, T.; Aro, N.; Ilmen, M.; Munoz, G.; Kalkkinen, N.; Penttila, M. *Eur J Biochem* **1997**, *248*, 415.

(3) Aimanianda, V.; Bayry, J.; Bozza, S.; Kniemeyer, O.; Perruccio, K.; Elluru, S. R.; Clavaud, C.; Paris, S.; Brakhage, A. A.; Kaveri, S. V.; Romani, L.; Latge, J. P. *Nature* **2009**, *460*, 1117.

(4) Wessels, J. G. H. *Annual Review of Phytopathology* **1994**, *32*, 413.

(5) Nakari-Setala, T.; Aro, N.; Kalkkinen, N.; Alatalo, E.; Penttila, M. *Eur J Biochem* **1996**, *235*, 248.

(6) Lugones, L. G.; Bosscher, J. S.; Scholtmeyer, K.; de Vries, O. M.; Wessels, J. G. *Microbiology* **1996**, *142 (Pt 5)*, 1321.

(7) De Vries, O. M.; Moore, S.; Arntz, C.; Wessels, J. G.; Tudzynski, P. *Eur J Biochem* **1999**, *262*, 377.

(8) Askolin, S.; Linder, M.; Scholtmeijer, K.; Tenkanen, M.; Penttila, M.; de Vocht, M. L.; Wosten, H. A. *Biomacromolecules* **2006**, *7*, 1295.

(9) Lugones, L. G.; Wosten, H. A.; Wessels, J. G. *Microbiology* **1998**, *144 (Pt 8)*, 2345.

(10) Lugones, L. G.; Scholtmeijer, K.; Klootwijk, R.; Wessels, J. G. *Mol Microbiol* **1999**, *32*, 681.

(11) Scholtmeijer, K.; Janssen, M. I.; Gerssen, B.; de Vocht, M. L.; van Leeuwen, B. M.; van Kooten, T. G.; Wosten, H. A.; Wessels, J. G. *Appl Environ Microbiol* **2002**, *68*, 1367.

(12) Anonymous *Chem Eng News* **2008**, *86*, 18.

(13) Linder, M. B. *Curr Opin Colloid In* **2009**, *14*, 356.

(14) Wosten, H.; De Vries, O.; Wessels, J. *Plant Cell* **1993**, *5*, 1567.

(15) Starov, V. M.; Velarde, M. G.; Radke, C. J. *Wetting and spreading dynamics*; CRC Press: Boca Raton, 2007.

(16) Pashley, R. M.; Karaman, M. E. *Applied colloid and surface chemistry*; J. Wiley: Chichester, West Sussex, England ; Hoboken, N.J., 2004.

(17) Bhushan, B.; Jung, Y. C. *Prog Mater Sci* **2011**, *56*, 1.

(18) Tadmor, R. *Langmuir* **2004**, *20*, 7659.

(19) Chandler, D. *Nature* **2005**, *437*, 640.

(20) Extrand, C. W. *Langmuir* **2003**, *19*, 3793.
(21) Marmur, A. *Langmuir* **2003**, *19*, 8343.
(22) Neinhuis, C.; Barthlott, W. *Ann Bot-London* **1997**, *79*, 667.
(23) Wagner, P.; Furstner, R.; Barthlott, W.; Neinhuis, C. *J Exp Bot* **2003**, *54*, 1295.
(24) Gao, X.; Jiang, L. *Nature* **2004**, *432*, 36.
(25) Yang, B.; Gao, X. F.; Yan, X.; Yao, X.; Xu, L.; Zhang, K.; Zhang, J. H.; Jiang, L. *Adv Mater* **2007**, *19*, 2213.
(26) Rabe, M.; Verdes, D.; Seeger, S. *Adv Colloid Interface Sci* **2011**, *162*, 87.
(27) Norde, W. *Macromol Symp* **1996**, *103*, 5.
(28) Jones, K. L.; O'Melia, C. R. *J Membrane Sci* **2000**, *165*, 31.
(29) Andrade, J. D.; Hlady, V.; Wei, A. P. *Pure Appl Chem* **1992**, *64*, 1777.
(30) Linder, M. B.; Szilvay, G. R.; Nakari-Setala, T.; Penttila, M. E. *FEMS Microbiol Rev* **2005**, *29*, 877.
(31) Kyte, J.; Doolittle, R. F. *J Mol Biol* **1982**, *157*, 105.
(32) Wösten, H. A.; Willey, J. M. *Microbiology* **2000**, *146 (Pt 4)*, 767.
(33) Bell-Pedersen, D.; Dunlap, J. C.; Loros, J. J. *Genes Dev* **1992**, *6*, 2382.
(34) Stringer, M. A.; Dean, R. A.; Sewall, T. C.; Timberlake, W. E. *Genes Dev* **1991**, *5*, 1161.
(35) Thau, N.; Monod, M.; Crestani, B.; Rolland, C.; Tronchin, G.; Latge, J. P.; Paris, S. *Infection and Immunity* **1994**, *62*, 4380.
(36) Temple, B.; Horgen, P. A.; Bernier, L.; Hintz, W. E. *Fungal Genet Biol* **1997**, *22*, 39.
(37) Askolin, S.; Penttila, M.; Wosten, H. A.; Nakari-Setala, T. *FEMS Microbiol Lett* **2005**, *253*, 281.
(38) Keyhani, N. O.; Zhang, S. Z.; Xia, Y. X.; Kim, B. *Molecular Microbiology* **2011**, *80*, 811.
(39) van Wetter, M. A.; Wosten, H. A.; Wessels, J. G. *Mol Microbiol* **2000**, *36*, 201.
(40) van Wetter, M. A.; Wosten, H. A.; Sietsma, J. H.; Wessels, J. G. *Fungal Genet Biol* **2000**, *31*, 99.
(41) De Groot, P. W.; Schaap, P. J.; Sonnenberg, A. S.; Visser, J.; Van Griensven, L. J. *J Mol Biol* **1996**, *257*, 1008.
(42) Talbot, N. J. *Nature* **1999**, *398*, 295.
(43) Israelachvili, J. N. *Intermolecular and surface forces*; 2nd ed. ed.; Academic, 1991.
(44) Lumsdon, S. O.; Green, J.; Stieglitz, B. *Colloids Surf B Biointerfaces* **2005**, *44*, 172.
(45) Cox, A. R.; Cagnol, F.; Russell, A. B.; Izzard, M. J. *Langmuir* **2007**, *23*, 7995.
(46) de Vocht, M. L.; Scholtmeijer, K.; van der Vegte, E. W.; de Vries, O. M.; Sonveaux, N.; Wosten, H. A.; Ruysschaert, J. M.; Hadziloannou, G.; Wessels, J. G.; Robillard, G. T. *Biophys J* **1998**, *74*, 2059.
(47) Sarlin, T.; Nakari-Setala, T.; Linder, M.; Penttila, M.; Haikara, A. *J I Brewing* **2005**, *111*, 105.
(48) Szilvay, G. R.; Nakari-Setala, T.; Linder, M. B. *Biochemistry* **2006**, *45*, 8590.
(49) Szilvay, G. R.; Paananen, A.; Laurikainen, K.; Vuorimaa, E.; Lemmetyinen, H.; Peltonen, J.; Linder, M. B. *Biochemistry* **2007**, *46*, 2345.

(50) Kisko, K.; Szilvay, G. R.; Vainio, U.; Linder, M. B.; Serimaa, R. *Biophys J* **2008**, *94*, 198.

(51) Kisko, K.; Szilvay, G. R.; Vuorimaa, E.; Lemmetyinen, H.; Linder, M. B.; Torkkeli, M.; Serimaa, R. *Langmuir* **2009**, *25*, 1612.

(52) Hakanpaa, J.; Paananen, A.; Askolin, S.; Nakari-Setala, T.; Parkkinen, T.; Penttila, M.; Linder, M. B.; Rouvinen, J. *J Biol Chem* **2004**, *279*, 534.

(53) Hakanpaa, J.; Szilvay, G. R.; Kaljunen, H.; Maksimainen, M.; Linder, M.; Rouvinen, J. *Protein Sci* **2006**, *15*, 2129.

(54) Whiteford, J. R.; Spanu, P. D. *Mol Plant Pathol* **2002**, *3*, 391.

(55) Wang, Z.; Lienemann, M.; Qiau, M.; Linder, M. B. *Langmuir* **2010**, *26*, 8491.

(56) Hou, S.; Yang, K.; Qin, M.; Feng, X. Z.; Guan, L.; Yang, Y.; Wang, C. *Biosens Bioelectron* **2008**, *24*, 918.

(57) Li, X.; Hou, S.; Feng, X.; Yu, Y.; Ma, J.; Li, L. *Colloids Surf B Biointerfaces* **2009**, *74*, 370.

(58) Valo, H. K.; Laaksonen, P. H.; Peltonen, L. J.; Linder, M. B.; Hirvonen, J. T.; Laaksonen, T. J. *ACS Nano* **2010**, *4*, 1750.

(59) Scholtmeijer, K.; Akanbi, M. H. J.; Post, E.; Meter-Arkema, A.; Rink, R.; Robillard, G. T.; Wang, X. Q.; Wosten, H. A. B. *Colloid Surface B* **2010**, *75*, 526.

(60) Janssen, M. I.; van Leeuwen, M. B.; Scholtmeijer, K.; van Kooten, T. G.; Dijkhuizen, L.; Wosten, H. A. *Biomaterials* **2002**, *23*, 4847.

(61) Misra, R.; Li, J.; Cannon, G. C.; Morgan, S. E. *Biomacromolecules* **2006**, *7*, 1463.

(62) Kurppa, K.; Jiang, H.; Szilvay, G. R.; Nasibulin, A. G.; Kauppinen, E. I.; Linder, M. B. *Angew Chem Int Ed Engl* **2007**, *46*, 6446.

(63) Laaksonen, P.; Kainlauri, M.; Laaksonen, T.; Shchepetov, A.; Jiang, H.; Ahopelto, J.; Linder, M. B. *Angew Chem Int Ed Engl* **2010**, *49*, 4946.

(64) Linder, M.; Selber, K.; Nakari-Setala, T.; Qiao, M.; Kula, M. R.; Penttila, M. *Biomacromolecules* **2001**, *2*, 511.

(65) Paananen, A.; Vuorimaa, E.; Torkkeli, M.; Penttila, M.; Kauranen, M.; Ikkala, O.; Lemmetyinen, H.; Serimaa, R.; Linder, M. B. *Biochemistry* **2003**, *42*, 5253.

(66) Ulman, A. *Chem Rev* **1996**, *96*, 1533.

(67) Witt, D.; Klajn, R.; Barski, P.; Grzybowski, B. A. *Curr Org Chem* **2004**, *8*, 1763.